BAZ2A-RNA mediated association with TOP2A and KDM1A represses gene expression in prostate cancer

Marcin Roganowicz[1,2], Dominik Bär[2] and Raffaella Santoro[2*]

1. Department of Molecular Mechanisms of Disease, DMMD, University of Zurich, 8057 Zurich, Switzerland
2. RNA Biology Program, Life Science Zurich Graduate School, University of Zurich, 8057 Zurich, Switzerland

* Corresponding author:
Raffaella Santoro (raffaella.santoro@dmmd.uzh.ch)

Abstract

BAZ2A is the epigenetic repressor of rRNA genes that are transcribed by RNA Polymerase I. In prostate cancer (PCa), however, BAZ2A function was shown to go beyond this role since it can also repress other genes that are frequently silenced in metastatic disease. However, the mechanisms of BAZ2A-mediated repression in PCa remain elusive. Here we show that BAZ2A represses genes implicated in PCa through its RNA-binding TAM domain using mechanisms that differ from the silencing of rRNA genes. While TAM domain mediates BAZ2A recruitment to rRNA genes, in PCa cells TAM domain is not required for the association with BAZ2A-regulated genes. Instead, BAZ2A-TAM domain in association with RNA mediates the interaction with the topoisomerase 2A (TOP2A) and the histone demethylase KDM1A, which have been previously implicated in aggressive PCa. TOP2A and KDM1A expression levels positively correlate with BAZ2A levels in both localized and aggressive PCa. Pharmacological inhibition of TOP2A and KDM1A activity upregulates the expression of BAZ2A-repressed genes implicated in PCa that are regulated by a class of inactive enhancers bound by BAZ2A. Our findings indicate that RNA-mediated interactions between BAZ2A and TOP2A and KDM1A regulate gene expression in PCa and may prove to be useful for the stratification of prostate cancer risk and treatment in patients.

Introduction

Prostate cancer (PCa) is the second most frequent cancer in men and the fifth leading cause of cancer death (Sung et al., 2021). Most of the PCa are indolent ones, with no threat to mortality, however, in many cases an aggressive form of disease develops and progresses to metastasis, which accounts for almost two thirds of prostate cancer-related deaths (Siegel et al., 2015). PCa displays a high heterogeneity that leads to distinct histopathological and molecular features (Li and Shen, 2018). This heterogeneity posits one of the most confounding and complex factors underlying its diagnosis, prognosis, and treatment (Yadav et al., 2018).

BAZ2A (also known as TIP5) is a chromatin regulator that has been shown to be implicated in aggressive PCa (Gu et al., 2015; Pietrzak et al., 2020). BAZ2A is a critical epigenetic regulator of PCa, is highly expressed in metastatic PCa, and involved in maintaining PCa cell growth and repressing genes frequently silenced in metastatic PCa (Gu et al., 2015). Elevated BAZ2A level indicates poor outcome (Pietrzak et al., 2020) and is also of high prognostic value for predicting PCa recurrence (Gu et al., 2015). However, the mechanisms of how BAZ2A mediates gene repression in PCa remain yet elusive.

Studies in mouse non-cancer and differentiated cells showed that BAZ2A is the epigenetic repressor of the ribosomal (r)RNA genes that are transcribed by RNA Polymerase I (Pol I) (Santoro et al., 2002). BAZ2A contains a TAM (TIP5/ARBD/MBD) domain that was shown to specifically interact with the long non-coding (lnc) promoter (p)RNA (Anosova et al., 2015; Guetg et al., 2012; Mayer et al., 2006). This transcript originating from an alternative promoter of the rRNA genes is required for BAZ2A interaction with the transcription termination factor I (TTF1) bound to the promoter of rRNA genes, thereby mediating BAZ2A recruitment and transcriptional silencing (Leone et al., 2017; Savic et al., 2014). While in non-cancer and differentiated cells BAZ2A is mainly located in the nucleolus, where it represses rRNA genes, BAZ2A function in PCa goes beyond this nucleolar function since it localizes in the entire nucleoplasm and also represses Pol II transcribed genes that are frequently silenced in metastatic PCa (Gu et al., 2015; Peña-Hernández et al., 2021). However, whether in PCa cells BAZ2A uses similar mechanisms to repress genes transcribed by Pol I (i.e. rRNA genes) and Pol II remains unclear.

In this work, we show that BAZ2A represses the expression of genes implicated in PCa through its RNA-binding TAM domain by using mechanisms that differ from the silencing of rRNA genes. We found that rRNA gene expression in PCa cells is still affected by pRNA and BAZ2A, indicating a conserved mechanism of rRNA gene silencing between different species and cell types. In contrast, Pol II BAZ2A-regulated genes are not affected by pRNA. Further, BAZ2A-TAM domain is not required for the recruitment to Pol II target genes. Instead, TAM domain mediates BAZ2A association with factors implicated in the regulation of gene expression, chromatin organization, nuclear pore complex, and RNA splicing. Among BAZ2A-TAM dependent interacting proteins, we found the topoisomerase 2A (TOP2A) and the histone demethylase KDM1A, which have been previously implicated in aggressive PCa (Labbé et al., 2017a; Liang et al., 2017; Sehrawat et al., 2018). TOP2A and BAZ2A expression levels positively correlates with BAZ2A levels in both localized and aggressive PCa. Importantly, BAZ2A interaction with TOP2A and KDM1A requires RNA. Further, pharmacological inhibition of TOP2A and KDM1A activity upregulates the expression of BAZ2A-repressed genes that are regulated by a class of inactive enhancers bound by BAZ2A. Our findings indicate that RNA-mediated interactions between BAZ2A and TOP2A and KDM1A are implicated in PCa and may prove to be useful for the stratification of prostate cancer risk and treatment in patients.

Results

BAZ2A-TAM domain mediates BAZ2A-RNA interaction and the association with the chromatin in PC3 cells

Previous results showed that the function of BAZ2A goes beyond the silencing of rRNA genes since it can also repress the expression of Pol II transcribed genes linked to PCa (Gu et al., 2015; Peña-Hernández et al., 2021). In BAZ2A-mediated rRNA gene silencing, BAZ2A-TAM domain plays an important role since its interaction with the lncRNA pRNA is required for BAZ2A recruitment to the promoter of rRNA genes (Leone et al., 2017; Mayer et al., 2006; Savic et al., 2014). To determine whether BAZ2A represses the expression of Pol II transcribed genes in PCa using mechanisms similar to rRNA gene silencing, we analysed the role of BAZ2A-TAM domain in PCa cells. We first investigated whether BAZ2A can interact

with RNA in PCa cells. We irradiated metastatic PCa PC3 cells with ultraviolet (UV) light that promotes the formation of covalent bonds between RNA binding proteins (RBPs) and their direct RNA binding sites (Lee and Ule, 2018) (**Fig. 1a**). We performed HA-immunoprecipitation (IP) using a previously established PC3 cell line that expresses endogenous BAZ2A tagged with FLAG-HA (H/F-BAZ2A-PC3) (Peña-Hernández et al., 2021) followed by ^{32}P-radiolabelling of RNA (**Fig. 1a**). As control, we performed HA-IPs with wild-type (WT) PC3 cells and F/H-BAZ2A-PC3 cells that were not UV-irradiated. Although similar amounts of H/F-BAZ2A were immunoprecipitated from irradiated and not irradiated F/H-BAZ2A-PC3 cells, radioactive RNA signal could only be detected in F/H-BAZ2A from UV cross-linked cells and this signal was reduced upon treatment with high RNase I amount, indicating that BAZ2A directly interacts with RNA in PC3 cells. To determine whether the interaction with RNA is mediated by BAZ2A-TAM domain, we performed HA-immunoprecipitation with UV-irradiated PC3 cells transfected with plasmids expressing H/F-BAZ2A wild-type (WT) or -BAZ2A$_{WY/GA}$ mutant that previous work showed to have a reduced binding affinity for RNA (Anosova et al., 2015; Guetg et al., 2012; Mayer et al., 2006) (**Fig. 1b**). We found that immunoprecipitated BAZ2A$_{WT}$ displays a stronger RNA radioactive signal compared to BAZ2A$_{WY/GA}$, indicating that BAZ2A-RNA interaction in PC3 cells occurs through BAZ2A-TAM domain. Taken together, these results indicate that in PCa cells the TAM domain is required for BAZ2A-interaction with RNA. We performed individual-nucleotide resolution Cross-Linking and ImmunoPrecipitation (iCLIP) to identify RNAs interacting with BAZ2A in PC3 cells, however, the libraries we obtained did not have sufficient quality for downstream analyses. Thus, we tested whether pRNA, the known BAZ2A-intercating RNA (Mayer et al., 2006), could affect the expression of known BAZ2A-regulated genes in PCa cells (Gu et al., 2015). We co-transfected PC3 cells with constructs expressing a RNA-control or pRNA under the control of the human rRNA gene promoter and GFP under the control of EF-1α promoter and isolated GFP(+)-cells by FACS sorting 72 hours later (**Fig. 1c**). Consistent with previous results, the overexpression of pRNA caused downregulation of 45S pre-rRNA, indicating that pRNA regulates rRNA gene expression in PCa cells as well (Mayer et al., 2006) (**Fig. 1d**). In contrast, pRNA did not cause significant changes in the expression of Pol II BAZ2A-regulated genes, indicating that their regulation is pRNA independent. These results suggest that

BAZ2A represses these genes using mechanisms that differ from the silencing of rRNA genes that require pRNA.

BAZ2A regulates a set of genes involved in PCa through its TAM domain

To determine whether BAZ2A-mediated gene regulation in PCa cells depends on the TAM domain, we performed RNAseq analysis on PC3 cells expressing $BAZ2A_{WT}$ and $BAZ2A_{\Delta TAM}$. We engineered all-in-one constructs that express F/H-tagged mouse $BAZ2A_{WT}$ (F/H-$mBAZ2A_{WT}$) or $BAZ2A_{\Delta TAM}$ (F/H-$mBAZ2A_{\Delta TAM}$) under CMV promoter, the GFP reporter gene under EF-1α promoter, and shRNA against human (h)BAZ2A sequences that do not target m*BAZ2A* sequences (**Fig. 2a**). hBAZ2A and mBAZ2A share high sequency homology (86%) and identical TAM domain sequences. The expression of shRNA that specifically targets hBAZ2A was reasoned to obtain mBAZ2A expression with simultaneous downregulation of the endogenous hBAZ2A. We transfected PC3 cells with the all-in-one constructs and isolated GFP(+)-cells by FACS sorting 72 hours later. We confirmed equal expression of $mBAZ2A_{WT}$ and $mBAZ2A_{\Delta TAM}$ by western blot (**Fig. 2b**) and the reduction of endogenous hBAZ2A by qRT-PCR in FACS-sorted GFP(+) PC3 cells (**Fig. 2c**). Correlation analysis clustered separately PCa cells expressing $mBAZ2A_{\Delta TAM}$ or $mBAZ2A_{WT}$, indicating a differential gene expression profile (**Fig. 2d**). We identified 118 upregulated genes and 545 downregulated genes in PC3 cells expressing $mBAZ2A_{\Delta TAM}$ compared to cells expressing $mBAZ2A_{WT}$ ($\log_2$ fold change ±0.58, $P < 0.05$, **Fig. 2e**). We validated some known genes that were previously shown to be repressed by BAZ2A in PCa (Gu et al., 2015) and found that they were significantly upregulated in cells expressing $mBAZ2A_{\Delta TAM}$ compared to PC3 cell expressing $mBAZ2A_{WT}$ or only GFP (**Fig. 2f**). These results indicated that the repression of BAZ2A-regulated genes is dependent on BAZ2A-TAM domain but pRNA independent. The top GO terms for the upregulated genes were related to tissue and organ development, cell migration and locomotion, regulation of epithelial cells proliferation and angiogenesis (**Fig. 2g**). Many of these processes are recognized as hallmarks of cancer, such as proliferative signalling, angiogenesis induction, and activation of invasion and metastasis (Hanahan and Weinberg, 2011; Zhong et al., 2020). The GO terms for downregulated genes were mostly related to metabolic processes that are also known to contribute to various cancers

development by fuelling cancer cells growth and division (Hanahan and Weinberg, 2011). All these results indicate that BAZ2A regulates the expression of genes implicated in cancer-related processes through its TAM domain.

TOP2A and KDM1A associate with BAZ2A via TAM domain and RNA and regulate the expression of BAZ2A-repressed genes in PC3 cells

Previous BAZ2A-ChIPseq analyses in PC3 cells determined that BAZ2A associates with a class of inactive enhancers that are enriched in histone H3 acetylated at Lysin 14 (H3K14ac) and depleted of H3K27ac and H3K4me1 (Peña-Hernández et al., 2021). This group of inactive enhancers was termed as class 2 (C2)-enhancers. The interaction of BAZ2A with C2-enhancers was shown to be mediated by the BAZ2A-bromodomain that specifically binds to H3K14ac. Importantly, genes in the nearest linear proximity to BAZ2A-bound C2-enhancers were repressed by BAZ2A, indicating that BAZ2A represses gene expression through the association with this class of inactive enhancers. To determine whether BAZ2A-TAM domain is required for the repression of these genes, we analysed the RNAseq profiles of PC3 cells expressing $BAZ2A_{WT}$ and $BAZ2A_{\Delta TAM}$ and found that 25% (240) of the genes in the nearest linear proximity to BAZ2A-bound C2-enhancers were significantly affected by $BAZ2A_{\Delta TAM}$ compared to $BAZ2A_{WT}$ (**Fig. 3a,b**). Remarkably, the majority of these BAZ2A-TAM regulated genes (202, 84%) were significantly upregulated upon the expression of $BAZ2A_{\Delta TAM}$, suggesting a major role of BAZ2A-TAM domain in repressing gene transcription through its interaction with C2-enhancers. The top GO terms of these genes were linked to signal transduction, response to wounding and cell migration and motility (**Fig. 3c**). Interestingly, the analysis of a comprehensive dataset comparing gene expression between metastatic tumours to normal tissue showed that many genes upregulated by $BAZ2A_{\Delta TAM}$ and implicated in signal transduction and cell motility are repressed in metastatic PCa.

Since the TAM domain was shown to be required for BAZ2A association with rRNA genes (Mayer et al., 2006), we asked whether this was also the case for BAZ2A interaction with C2-enhancers. We performed ChIP analysis of PC3 cells transfected with F/H-$mBAZ2A_{WT}$ or F/H-$mBAZ2A_{\Delta TAM}$ and analysed BAZ2A association with C2-enhancers that were close to genes upregulated by $BAZ2A_{\Delta TAM}$. However, we did not find any significant alterations in the binding

of BAZ2A$_{\Delta TAM}$ with these regions relative to BAZ2A$_{WT}$ (**Fig. 3d**). Similarly, the interaction with the promoter of AOX1, a known BAZ2A-regulated gene (Gu et al., 2015; Peña-Hernández et al., 2021), was not affected. These results indicate that the interaction with these target loci is not mediated by BAZ2A-TAM domain. Further, they support previous data showing that it is the BAZ2A-BRD domain to be required for the interaction of these regions that are enriched in H3K14ac (Peña-Hernández et al., 2021). Consistent with previous results (Mayer et al., 2006), the ChIP analysis showed that the interaction of BAZ2A$_{\Delta TAM}$ with the promoter of rRNA genes was reduced compared to BAZ2A$_{WT}$ (**Fig. 3d**). Thus, while for rRNA gene silencing BAZ2A-TAM is required for the association with chromatin, in the case of Pol II genes BAZ2A-TAM domain is not necessary for the recruitment to target loci, suggesting different mechanisms by which BAZ2A represses gene expression in PCa cells.

Based on these results, we hypothesized that BAZ2A-TAM domain and its ability to interact with RNA might be important for the association with factors implicated in BAZ2A-mediated gene repression in PCa cells. To test this, we performed HA-IP combined with mass-spec analysis from PC3 cells transfected with plasmids expressing F/H-BAZ2A$_{WT}$ and the deficient RNA-binding mutant F/H-BAZ2A$_{WY/GA}$. The IP specificity was validated by western blot with antibodies against HA to detect F/H-BAZ2A and against SNF2H, a well-known BAZ2A-interacting protein (Dalcher et al., 2020; Strohner et al., 2001) (**Fig. 4a**). We defined BAZ2A$_{WT}$-interacting proteins those factors showing in all the three replicates at least two peptides and ≥ 2 fold peptide number in IPs with H/F-BAZ2A$_{WT}$ relative to IPs from cells transfected with empty vector. To identify factors that specifically associate with BAZ2A through a functional BAZ2A-TAM domain, we considered BAZ2A$_{WT}$-intercating proteins that showed ≥ 2 fold peptide number in IPs with H/F-BAZ2A$_{WT}$ relative to IPs with BAZ2A$_{WY/GA}$ in at least two replicates (**Fig. 4b**). Using these criteria, proteins previously shown to interact with BAZ2A independently of RNA, such as SNF2H and DHX9, showed similar binding with both BAZ2A$_{WT}$ and BAZ2A$_{WY/GA}$ (Leone et al., 2017) (**Fig. 4b**). We identified 74 proteins that had decreased association with BAZ2A$_{WY/GA}$ compared to BAZ2A$_{WT}$. We applied the Search Tool for the Retrieval of Interacting Genes/Proteins database (STRING) (Szklarczyk et al., 2015) and found that proteins with decreased association with BAZ2A$_{WY/GA}$ were involved in pathways linked to the regulation of gene expression, chromosome organization, nuclear pore

complex organization, and RNA processing (**Fig. 4b**). Amongst them, we found factors that regulate transcription and topological states of DNA such as topoisomerase 2A and 2B (TOP2A and TOP2B), histone demethylase KDM1A (also known as LSD1) and several components of cohesin protein complex (SMC1A, RAD21, STAG2). We also observed loss of BAZ2A interactions with factors involved in RNA processing and splicing (CTNNBL1, EFTUD2) and nuclear pore complex formation (NUP107, NUP133, NUP97). We validated the dependency of BAZ2A-TAM domain for BAZ2A-interaction with TOP2A, SMC1A, RAD21, NUP107, and KDM1A by anti-HA IP of PC3 cells transfected with plasmids expressing H/F-mBAZ2A$_{WT}$, -mBAZ2A$_{WY/GA,}$ and -mBAZ2A$_{\Delta TAM}$ followed by western blot (**Fig. 4d**). We confirmed these interactions also with endogenous BAZ2A by performing HA-IP in PC3 cells expressing endogenous tagged with HA and FLAG sequences (H/F-BAZ2A) (**Fig. 4e**). To determine whether these BAZ2A-interactions are mediated by the TAM domain itself or RNA bound to the TAM domain, we treated nuclear extracts of PC3$_{wt}$ and F/H-BAZ2A-PC3 cells with RNase A and found that TOP2A and KDM1A association with BAZ2A was strongly reduced (**Fig. 4e**). In contrast, BAZ2A-association with RAD21, SMC1A, and NUP107 were not affected by RNase A, suggesting that these interactions are BAZ2A-TAM-dependent but RNA independent (**Fig. 4f**). These results indicated that BAZ2A-TAM domain mediates alone or in combination with RNA the interaction with proteins mainly involved in chromatin regulation. Further, they show that RNA may act as a scaffold for the association of BAZ2A with TOP2A and KDM1A.

Previous studies have implicated both TOP2A and KDM1A in PCa. Elevated expression of KDM1A was shown to correlate with PCa recurrence (Kahl et al., 2006; Kashyap et al., 2013). Further, high TOP2A levels were significantly associated with increased risk of systemic progression in PCa patients (Cheville et al., 2008). Consistent with these results, the analyses of two data sets comparing normal tissue, localized tumor and metastatic PCa, revealed that *TOP2A* levels are highly elevated in metastatic PCa (Li et al., 2014) (**Fig. 5a,b**). This pattern is very similar to *BAZ2A* expression levels that were also found to be high in metastatic PCa (Gu et al., 2015). In contrast, the expression of *KDM1A* between metastatic PCa relative to localized tumor and normal tissue were less consistent between the two different datasets. The analysis of a large cohort of primary PCa and metastatic castration resistant PCa (CRPC)

(Cancer Genome Atlas Research, 2015; Robinson et al., 2015) revealed significantly higher expression of both *TOP2A* and *KDM1A* in tumours expressing high *BAZ2A* levels (quartile Q1: the top 25% of PCas with the highest BAZ2A expression) compared to tumours with low BAZ2A (quartile Q4: the top 25% of PCas with the lowest BAZ2A levels) (**Fig. 5c,d**). Further, the majority of primary PCa with high levels of *TOP2A* or *KDM1A* belong to the PCa subtype characterized by copy number alteration of the tumor suppressor gene *PTEN* and containing ERG fusion, that is the subtype charactering PCa with high BAZ2A expression (Pietrzak et al., 2020) (**Fig. 5e**). These results suggest that TOP2A and KDM1A might be functionally related with BAZ2A for the regulation of gene expression in PCa. To test this, we analysed whether TOP2A and KDM1A can affect the expression of BAZ2A-TAM regulated genes. We treated PC3 cells with the TOP2A inhibitor ICR-193 or the KDM1A inhibitor OG-L002 and measured the expression of eight genes that we found to be upregulated by $BAZ2A_{\Delta TAM}$ and were in the nearest linear proximity to BAZ2A-bound C2-enhancers (**Fig. 5f,g**). We found that 4 out of 8 analysed genes were significantly upregulated upon treatment with the TOP2A inhibitor ICR-193 (*MUC5B*, *HSPG2*, *CSF2*, *ZNF469*, **Fig. 5f**). Interestingly, these genes were also significantly upregulated upon treatment with the KDM1A inhibitor OG-L002 (**Fig. 5g**). In contrast, 45S pre-rRNA levels were not affected by both inhibitors. These results suggest that TOP2A and KDM1A through the RNA- and TAM-dependent association with BAZ2A regulate the expression of a set of genes implicated in PCa (**Fig. 5h**).

Discussion

Previous studies have implicated BAZ2A in aggressive PCa (Gu et al., 2015; Pietrzak et al., 2020), however, the mechanisms by which BAZ2A regulates gene expression in PCa cells remained elusive. In this work, we showed the importance of BAZ2A-TAM domain and its interaction with RNA in the regulation of gene expression of PCa cells.

Studies in mouse non-cancer and differentiated cells showed that BAZ2A-TAM domain associates with the lncRNA pRNA that is required for BAZ2A targeting and silencing of rRNA genes (Anosova et al., 2015; Guetg et al., 2012; Leone et al., 2017; Mayer et al., 2006). Here we show that the pRNA function in the regulation of rRNA gene silencing occurs in PCa as well, however, the expression of the other BAZ2A-regulated genes did not depend on pRNA.

Further, we confirmed that the TAM domain is important for targeting BAZ2A to rRNA genes (Mayer et al., 2006), however, we found that it is not required for its binding to the other BAZ2A-regulated genes. These results further support a role of BAZ2A in PCa that goes beyond the known regulation of rRNA gene transcription (Gu et al., 2015; Guetg et al., 2012; Santoro et al., 2002) and suggested different mechanisms by which BAZ2A represses gene expression in PCa cells.

We showed that BAZ2A-TAM domain is required for the repression of genes implicated in PCa. BAZ2A-TAM is not necessary for the interaction with target loci but serves for the association with several factors implicated in the regulation of gene expression, chromatin organization, nuclear pore complex, and RNA splicing. Recent work showed that BAZ2A recruitment to target loci, including C2 enhancers, is mainly mediated by its bromodomain that specifically interacts with H3K14ac. Mutations in the bromodomain abolishing the binding to H3K14ac impair BAZ2A binding to target loci, including the C2-enhancers (Peña-Hernández et al., 2021). These results indicate that BAZ2A regulation in PCa cells depends on both the bromo and the TAM domains; the bromodomain acts as an epigenetic reader targeting BAZ2A to chromatin regions enriched in H3K14ac whereas the TAM domain serves as scaffold for the recruitment of factors that impact gene expression (**Fig. 5h**).

Our results showed that BAZ2A associates with RNA in PCa cells, an interaction that is mediated by the TAM domain. Although we did not succeed to obtain iCLIP libraries with sufficient quality for the identification of BAZ2A-intercating RNAs, the data suggested that RNA is required for the interaction of BAZ2A with TOP2A and the histone demethylase KDM1A whereas other interacting proteins requiring BAZ2A-TAM domain, such as cohesin components, do not require RNA. Interestingly, the interaction of KDM1A with RNA has been previously reported by showing that the long intergenic noncoding RNAs (lincRNAs) HOTAIR serves as a scaffold that mediates the interaction of KDM1A and PRC2, thereby coordinating targeting of histone H3K27me3 and H3K4 demethylation on target genes (Tsai et al., 2010). Thus, by analogy, BAZ2A might recruit KDM1A through a yet unknown RNA to target sites. The reported ability of KDM1A to demethylate mono- and di-methylated lysine 4 of histone H3 (Rudolph et al., 2013) can probably serve to keep BAZ2A-bound C2-enhancers in an inactive state and thus contributing to gene repression. Accordingly, treatment of PC3 cells with

KDM1A inhibitors upregulated the expression of genes linked to inactive BAZ2A-bound C2-enhancers that are characterized by low H3K4me1 and H3K27ac levels (Peña-Hernández et al., 2021). KDM1A is highly expressed in various human malignancies and its activities were linked to carcinogenesis, making it a possible target for anticancer treatments (Maiques-Diaz and Somervaille, 2016). In particular, KDM1A was shown to promote the survival of CRPC by activating the lethal PCa gene network and supporting the proliferation of PCa cells (Liang et al., 2017; Sehrawat et al., 2018). Further, several inhibitors were recently shown to reduce the proliferative potential of PCa cells and prostate cancer growth (Etani et al., 2019; Yang et al., 2017). Thus, the association of KDM1A with BAZ2A defined novel mechanisms by which KDM1A can acts in PCa.

The other BAZ2A-TAM domain and RNA dependent associating factor is TOP2A. As in the case of KDM2A, also TOP2A has been reported to be frequently overexpressed in aggressive PCa and serves as an indicator of a poor outcome (Cheville et al., 2008; de Resende et al., 2013; Labbé et al., 2017b). Further, high levels of TOP2A were also found in CRPC (Hughes et al., 2006). Despite these correlations, however, the exact mechanism underlying the more aggressive phenotype associated with TOP2A is not known. Interestingly, BAZ2A-TOP2A interaction was previously detected in mouse embryonic stem cells (ESCs), where BAZ2A does not regulate rRNA gene expression (Dalcher et al., 2020). Similarly to PCa cells, BAZ2A and TOP2A in ESCs were shown to act together for the regulation of gene expression, suggesting that BAZ2A-TOP2A crosstalk is conserved among different species and cell types. It has been reported that TOP2A cooperates with androgen receptor (AR) to induce transcription of target genes, suggesting that androgen ablation therapy might be less effective in the presence of high level of TOP2A protein (Schaefer-Klein et al., 2015). In the case of BAZ2A, however, TOP2A activity seems to be related to gene repression, suggesting the TOP2A can act as activator or repressor depending on its interacting partners. The requirement of RNA for the association of TOP2A with BAZ2A suggested that TOP2A might be an RNA-binding protein. Consistent with this, recent high-resolution mapping of RNA-binding proteins detected a significant interaction of TOP2A with RNA (He et al., 2016; Mullari et al., 2017; Perez-Perri et al., 2018). However, it remains to be investigated whether RNA in general or a specific RNA can mediate the association of TOP2A with distinct complexes,

thereby specifying activating and/or repressing roles in gene expression. In conclusion, our findings indicate that RNA-mediated interactions between BAZ2A and TOP2A and KDM1A are implicated in PCa and may prove to be useful for the stratification of prostate cancer risk and treatment in patients.

Acknowledgement

We thank Rostyslav Kuzyakiv for help in bioinformatic analyses. We thank Peter Hunziker, Catherine Aquino, and the Functional Genomic Center Zurich for the assistance in sequencing and proteomic analysis. This work was supported by the the National Center of Competence in Research RNA & Disease (funded by the SNSF), Swiss National Science Foundation (31003A-173056), Forschungskredit of the University of Zurich (to M.R.), Olga Mayenfisch Stifung, Krebsliga Zurich, Swiss Cancer Research Foundation (KFS-4527-08-2018-R), and ERC grant (ERC-AdG-787074-NucleolusChromatin).

Dataset

All raw data generated in this paper using high throughput sequencing are accessible through National Center for Biotechnology Information Gene Expression Omnibus (GEO) database, https://www.ncbi.nlm.nih.gov/geo (accession no. GSE179743).

Conflict of interest

The authors declare they have no conflict of interest.

Material and Methods

Culture of PC3 cells

The PC3 cell line was purchased from the American Type Culture Collection. PC3 cells were cultured in RPMI 1640 medium and Ham's F12 medium (1:1; Gibco) containing 10% FBS (Gibco) and 1% penicillin-streptomycin (Gibco). $2.5x10^6$ cells were seeded in 150 mm tissue culture dishes (TPP®) and cultured for 2 to 3 days. All cells were regularly tested for mycoplasma contamination. The F/H-BAZ2A PC3 cell line was described in (Peña-Hernández et al., 2021)

Construct design

cDNA corresponding to HA-FLAG tagged mouse wild type BAZ2A (H/F-$BAZ2A_{WT}$), CopGFP and shBAZ2A for human BAZ2A were cloned into DC-DON-SH01 vector (GeneCopoeia). Site-directed mutagenesis was performed to create BAZ2A mutants WY531/532GA (H/F-$BAZ2A_{WY/GA}$) and ΔTAM (HA/FLAG-$BAZ2A_{\Delta TAM}$). The sequencing of plasmids was performed to ensure fidelity of sequences.

Plasmid transfections

$1x10^6$ of PC3 cells were seeded in 100 mm culture dish (TPP®), grown for 24 hours and transfected with 8 µg of plasmids and 8 µl of X-tremeGENE HP DNA Transfection Reagent (Roche). The cells were grown for 48 hours post-transfection and collected for downstream analyses.

RNA extraction, reverse transcription, and quantitative PCR

RNA was purified with TRIzol reagent (Life Technologies). 1µg total RNA was primed with random hexamers and reverse-transcribed into cDNA using MultiScribe™ Reverse Transcriptase (Life Technologies). Amplification of samples without reverse transcriptase assured absence of genomic or plasmid DNA (data not shown). The relative transcription levels were determined by normalization to *GAPDH or β-actin* mRNA levels, as indicated. qRT-PCR was performed with KAPA SYBR® FAST (Sigma) on Rotor-Gene RG-3000 A (Corbett Research).

Treatment of PC3 cells with ICRF-193 and LG-001

$1x10^6$ PC3 cells were seeded in 100 mm culture dish (TPP®), 24 hours prior to the treatment. ICRF-193 (Sigma) or OG-L002 (MedChemExpress) were added directly to the medium to obtain a final 10 µM concentration. Cells were harvested for downstream analyses 48 hours after treatment with the inhibitors.

Chromatin immunoprecipitation

ChIP experiments were performed as previously described (Leone et al., 2017; Peña-Hernández et al., 2021). Briefly, 1% formaldehyde was added to cultured cells to cross-link proteins to DNA. Isolated nuclei were then digested with MNase (S7 Micrococcal nuclease, Roche) and briefly sonicated using a Bioruptor ultrasonic cell disruptor (Diagenode) to shear genomic DNA to an average fragment size of 200 bp. 200 µg of chromatin was diluted tenfold with ChIP buffer (16.7 mM Tris-HCl pH 8.1, 167 mM NaCl, 1.2 mM EDTA, 0.01% SDS and 1.1% Triton X-100) and precleared for 2h with 10 µl of packed Sepharose beads for at least 2h at 4°C. Immunoprecipitation was done overnight with the HA-magnetic beads (Pierce™ Anti-HA magnetic beads, ThermoFisher Scientific). After washing, elution and reversion of cross-links, eluates were treated with RNAse A (1µg). DNA was purified with phenol-chloroform, ethanol precipitated and quantified by quantitative PCR.

RNAseq and data analysis

$1.5x10^5$ PC3 cells were seeded into each well of a 6-well culture dish (TPP®), grown for 24 hours, and transfected with constructs expressing either H/F-BAZ2A$_{WT}$ or H/F-BAZ2A$_{\Delta TAM}$ with simultaneous downregulation of endogenous human BAZ2A. 4 µg of plasmid and 4 µl of X-tremeGENE HP DNA Transfection Reagent (Roche) were used per well. The cells were grown for 48 hours post-transfection, collected by trypsinization, and pooled. Using fluorescence activated cells sorting (FACS), the GFP(+) cells expressing H/F-BAZ2A$_{WT}$ or H/F-BAZ2A$_{\Delta TAM}$ were collected and their total RNA purified with TRIzol reagent (Life Technologies) as described above. Total RNA from 3 independent samples from PC3 cells expressing H/F-BAZ2A$_{WT}$ and from three independent samples expressing H/F-BAZ2A$_{\Delta TAM}$ were obtained. DNA contaminants were removed by treating RNA with 2U TURBO DNase I

(Invitrogen) for 1h at 37°C and the RNA samples were re-purified using TRIzol. The quality of the isolated RNA was determined by Bioanalyzer 2100 (Agilent, Waldbronn, Germany). Only those samples with a 260nm/280nm ratio between 1.8–2.1 and a 28S/18S ratio within 1.5–2 were further processed. The TruSeq RNA Sample Prep Kit v2 (Illumina, Inc, California, USA) was used in the succeeding steps. Briefly, total RNA samples (100-1000ng) were poly(A) enriched and then reverse-transcribed into double-stranded cDNA. The cDNA samples were fragmented, end-repaired and polyadenylated before ligation of TruSeq adapters containing the index for multiplexing. Fragments containing TruSeq adapters on both ends were selectively enriched with PCR. The quality and quantity of the enriched libraries were validated using Qubit® (1.0) Fluorometer and the Caliper GX LabChip® GX (Caliper Life Sciences, Inc., USA). The product was a smear with an average fragment size of approximately 260bp. The libraries were normalized to 10nM in Tris-Cl 10mM, pH8.5 with 0.1% Tween 20. The TruSeq SR Cluster Kit HS4000 (Illumina, Inc, California, USA) was used for cluster generation using 10pM of pooled normalized libraries on the cBOT. Sequencing was performed on the Illumina HiSeq 2500 single end 100bp using the TruSeq SBS Kit HS2500 (Illumina, Inc, California, USA). Reads were aligned to the reference genome (hg38) with Subread (i.e. subjunc, version 1.4.6-p4; (Liao et al., 2013)) allowing up to 16 alignments per read (options: –trim5 10 –trim3 15 -n 20 - m 5 -B 16 -H –allJunctions). Count tables were generated with Rcount (Schmid and Grossniklaus, 2015) and with an allocation distance of 10bp for calculating the weights of the reads with multiple alignments, considering the strand information, and a minimal number of 5 hits. Variation in gene expression was analyzed with a general linear model in R with the package edgeR (version 3.12.0; (Robinson and Oshlack, 2010)). Genes differentially expressed between specific conditions were identified with linear contrasts using trended dispersion estimates and Benjamini-Hochberg multiple testing corrections. Genes with a *P*-value below 0.05 and a minimal fold change of 1.5 were considered as differentially expressed. These thresholds have previously been used characterizing chromatin remodeler functions (de Dieuleveult et al., 2016). Gene ontology analysis was performed with David Bioinformatics Resource 6.8 (Huang da et al., 2009).

BAZ2A co-immunoprecipitation and mass spectrometric analysis

$1x10^6$ PC3 cells were seeded in 100 mm culture dish (TPP®), grown for 24 hrs and transfected with 8 µg of plasmid DNA for expression of HA/FLAG-BAZ2A$_{WT}$, HA/FLAG-BAZ2A$_{WY/GA}$ or HA/FLAG-BAZ2A$_{\Delta TAM}$. Four culture dishes were used per condition. Cells were grown for another 48 hours, harvested by scraping, and washed two times with PBS. Cells were then incubated for 10 min on ice in 3 ml of hypotonic buffer (10 mM HEPES pH 7.6, 1.5 mM $MgCl_2$, 10 mM KCl), spun down for 5 min, at 1000 g at 4°C, supplemented with 0.5% Triton X-100 and incubated for another 10 min at 4°C. Obtained nuclei were spun down for 10 min, at 1000 g at 4°C, resuspended in 500 µl of MNase digestion buffer (0.3 M Sucrose, 50 mM Tris–HCl pH 7.5, 30 mM KCl, 7.5 mM NaCl, 4 mM MgCl2, 1 mM CaCl2, 0.125% NP-40, 0.25% NaDeoxycholate) and supplemented with 50 U of MNase (Roche). Samples were incubated at 30 min at 37°C under shaking. Next the NaCl concentration was brought to 200 mM and samples were incubated for 10 min on ice. Samples were spun down at maximum speed, the pellets discarded, and 10% of the supernatant was collected as input samples. The remaining part of the supernatant was diluted four times with MNase buffer, supplemented with cOmpleteTM Protease Inhibitor Cocktail (Roche) and the samples were incubated overnight at 4°C with orbital shaking with 50 µl of HA magnetic beads (ThermoFisher Scientific) that were pre-washed three times with MNase buffer. The day after, the beads were washed three times for 30 min at 4°C with 1 ml of the wash buffer (20 mM HEPES pH 7.6, 20% glycerol, 200 mM NaCl, 1.5 mM $MgCl_2$, 0.2 mM EDTA, 0.02% NP-40). Half of the beads were further analyzed by Western Blotting whereas the other half was prepared for LC-MS/MS analyses. The dry beads were dissolved in 45 µl buffer containing 10 mM Tris + 2 mM $CaCl_2$, pH 8.2 and 5 µl of trypsin (100 ng/µl in 10 mM HCl) for digestion, which was carried out in a microwave instrument (Discover System, CEM) for 30 min at 5 W and 60°C. Samples were dried in a SpeedVac (Savant), dissolved in 0.1% formic acid (Romil), and an aliquot ranging from 5 to 25% was analyzed on a nanoAcquity UPLC (Waters Inc.) connected to a Q Exactive mass spectrometer (Thermo Scientific) equipped with a Digital PicoView source (NewObjective). Peptides were trapped on a Symmetry C18 trap column (5 µm, 180 µm × 20 mm, Waters Inc.) and separated on a BEH300 C18 column (1.7 µm, 75 µm × 150 m, Waters Inc.) at a flow rate of 250 nl/min using a gradient from 1% solvent

B (0.1% formic acid in acetonitrile, Romil)/99% solvent A (0.1% formic acid in water, Romil) to 40% solvent B/60% solvent A within 90 min. Mass spectrometer settings were as follows: Data-dependent analysis. Precursor scan range 350–1,500 m/z, resolution 70,000, maximum injection time 100 ms, threshold 3e6. Fragment ion scan range 200–2,000 m/z, Resolution 35,000, maximum injection time 120 ms, threshold 1e5. Proteins were identified using the Mascot search engine (Matrix Science, version 2.4.1). Mascot was set up to search the SwissProt database assuming the digestion enzyme trypsin. Mascot was searched with a fragment ion mass tolerance of 0.030 Da and a parent ion tolerance of 10.0 PPM. Oxidation of methionine was specified in Mascot as a variable modification. Scaffold (Proteome Software Inc.) was used to validate MS/MS-based peptide and protein identifications. Peptide identifications were accepted if they achieved a false discovery rate (FDR) of less than 0.1% by the Scaffold Local FDR algorithm. Protein identifications were accepted if they achieved an FDR of less than 1.0% and contained at least two identified peptides.

BAZ2A immunoprecipitation and RNA radiolabelling

$1x10^6$ of PC3 cells and $1x10^6$ H/F-BAZ2A PC3 cells were seeded in 150 mm culture dish (TPP®) and grown for 96 hours. Four dishes were used per condition. For the experiment performed with ectopically expressed H/F-BAZ2A$_{WT}$ and H/F-BAZ2A$_{WY/GA}$, $1x10^6$ PC3 cells were seeded in 100 mm culture dish (TPP®), grown for 24 hours and transfected with 8 µg of plasmid DNA. The proteins were expressed for 48 hours. Fifteen 100 mm dishes were used per condition.

Cells were washed with 5 ml of cold PBS, 2 ml of fresh and cold PBS was added and the cells were UV-B cross-linked with 400 mJ in UV-irradiator (Vilber). Cells were harvested by scraping, spun down at 1000 g for 5 min at 4°C, resuspended in 3 ml of the hypotonic buffer (10 mM HEPES pH 7.6, 1.5 mM $MgCl_2$, 10 mM KCl), and incubated for 15 min on ice. Next, cells were supplemented with 0.5% Triton X-100 and cOmpleteTM Protease Inhibitor Cocktail (Roche), incubated on ice for another 15 min and spun down at 1000 g for 5 min at 4°C. The pellet was resuspended in 500 µl of lysis buffer (50 mM TRIS-HCl pH 7.4, 100 mM NaCl, 0.1% SDS, 1% NP-40, 0.5% NaDeoxycholate) supplemented with cOmpleteTM Protease Inhibitor Cocktail (Roche) and incubated on ice for 10 min. 2 U of DNase (TURBO™ DNase,

ThermoFisher Scientific) and 0.02 U (high RNase treatment) or 0.0025 U (low RNase treatment) of RNase I (Ambion) was added to the lysates. Lysates were incubated at 37°C with shaking for exactly 2 min and immediately supplemented with 40 U of RNase inhibitor (RiboLock RNase Inhibitor, ThermoFisher Scientific) followed by 3 min incubation on ice. The NaCl concentration was brought to 400 mM followed by 10 min incubation at 4°C with orbital shaking. Samples were spun down at maximal speed for 5 min at 4°C and supplemented with 800 µl of no-salt lysis buffer (50 mM Tris-HCl pH 7.4, 0.1% SDS, 1% NP-40, 0.5% NaDeoxycholate), 40 U of RNase inhibitor and with cOmplete TM Protease Inhibitor Cocktail (Roche). For the input for Western blot analysis, 8% of each sample was taken and stored at -20°C. Samples were incubated overnight at 4°C with orbital shaking with 50 µl of HA magnetic beads (Pierce™ Anti-HA magnetic beads, ThermoFisher Scientific) pre-washed with no-salt lysis buffer. Beads were washed twice for 30 min at 4°C with 1 ml of high-salt wash buffer (50 mM Tris-HCl pH 7.4, 1 M NaCl, 1 mM EDTA, 1% NP-40, 0.1% SDS, 0.5% NaDeoxycholate) and once with low-salt wash buffer (20 mM Tris-HCl pH 7.4, 10 mM $MgCl_2$, 0.2% Tween-20). 10% of the beads were taken for Western blot analyses. The remaining beads were resuspended in 20 µl of the radiolabelling mixture (10U of T4 polynucleotides Kinase (Thermo Scientific), reaction buffer A (Thermo Scientific) and 5 µCi of [gamma-P^{32}]ATP (Hartmann Analytic)) and incubated for 10 min at 37°C with shaking. The supernatants were removed and the beads washed with 300 µl of low-salt lysis buffer. Samples were supplemented with 37 nM DTT and NuPAGE loading dye and incubated at 70°C for 10 min with shaking. Samples were spun down for 1 min at RT at max speed, the supernatants were loaded on 3-8% NuPAGE TRIS-Acetate gels (ThermoFisher Scientific) and run for 90 min at 150 V. The gels were transferred to the nitrocellulose membrane with iBLOT 2 Dry Blotting System (Invitrogen). The membrane containing radioactive samples was covered with light-sensitive film (Typox™) and exposed in darkness for 16 hours at -80°C.

BAZ2A co-immunoprecipitation with RNase treatment

$2x10^6$ of PC3 WT cells and $1x10^6$ H/F-BAZ2A PC3 cells were seeded in 150 mm culture dish (TPP®) and grown for 48 hrs. Five culture dishes were used per condition. Cells were harvested by scraping and washed two times with PBS. Cells were incubated for 10 min on

ice in 4 ml of hypotonic buffer (10 mM HEPES pH 7.6, 1.5 mM $MgCl_2$, 10 mM KCl), spun down for 5 min, at 1000 xg at 4°C, supplemented with 0.5% Triton X-100, and incubated for another 10 min at 4°C. Obtained nuclei were spun down for 10 min, at 1000 g at 4°C, resuspended in 500 µl of MNase digestion buffer (0.3 M Sucrose, 50 mM Tris–HCl pH 7.5, 30 mM KCl, 7.5 mM NaCl, 4 mM MgCl2, 1 mM CaCl2, 0.125% NP-40, 0.25% NaDeoxycholate) and supplemented with 40 U of MNase (Roche). Samples were shacked for 30 min at 37°C. Next, the NaCl concentration was brought to 200 mM and samples were incubated for 10 min on ice. Samples were spun down at maximum speed. The pellets were discarded and 10% of the supernatant was collected as an input and further analysed by Western blot. The remaining part of the supernatant was diluted four times with MNase buffer, supplemented with cOmpleteTM Protease Inhibitor Cocktail (Roche) and 100 µg/ml RNase A (ThermoFisher). The control samples were not treated with RNase A. The samples were incubated overnight at 4°C with orbital shaking with 25 µl of HA magnetic beads (Pierce™ Anti-HA magnetic beads, ThermoFisher Scientific) pre-washed three times with MNase buffer. The beads were washed three times for 30 min at 4°C with 1 ml of the wash buffer (20 mM HEPES ph 7.6, 20% glycerol, 200 mM NaCl, 1.5 mM $MgCl_2$, 0.2 mM EDTA, 0.02% NP-40) resuspended in a small volume of wash buffer. All the samples were loaded on a 6% home-made SDS-PAGE gel, run for 130 min at 120 V and analysed further by Western blot.

Figure legends

Figure 1

The TAM domain is required for BAZ2A binding to the RNA in PCa cells

a. BAZ2A interacts with RNA in PC3 cells. Top panel. Western blot showing anti-HA immunoprecipitates from $PC3_{WT}$ and H/F-BAZ2A PC3 cells irradiated with UV-light (UV X-linking) and treated with low (0.0025U) or high (0.02U) concentration of RNase I. BAZ2A signal was detected with anti-HA antibodies. Bottom panel. Autoradiography showing ^{32}P-radiolabeled-RNA from the indicated anti-HA immunoprecipitates.

b. BAZ2A interaction with RNA depend on TAM domain. Top panel. Western blot showing anti-HA immunoprecipitates from PC3 cells transfected with plasmids expressing H/F-$BAZ2A_{WT}$ and H/F-$BAZ2A_{WY/GA}$ that were UV-light irradiated and treated with 0.0025U RNase I. BAZ2A signal was detected with anti-BAZ2A antibodies. Bottom panel. Autoradiography showing ^{32}P-radiolabeled-RNA from the indicated anti-HA immunoprecipitates.

c. A scheme of the strategy used to measure gene expression in PC3 cells overexpressing the lncRNA pRNA.

d. qRT-PCR showing pRNA, 45S pre-rRNA and mRNA levels of tBAZ2A-regulated genes in GFP(+)-FACS-sorted PC3 cells. Transcript levels were normalized to *GAPDH* and cells transfected with RNA-control. Error bars represent standard deviation of three independent experiments. Statistical significance (*P*-value) was calculated using two-tailed t-test (**<0.01, ***< 0.001); ns: not significant.

Figure 2

BAZ2A regulates a set of genes involved in cancer development through its RNA-binding TAM domain

a. A scheme of the all-in-one plasmids for the expression of mouse HA-FLAG BAZ2A (H/F-mBAZ2A) under CMV promoter, GFP reporter gene under EF-1α promoter and shRNA for endogenous human BAZ2A under H1 promoter.

b. HA-BAZ2A immunoprecipitation from nuclear extracts of PC3 cells transfected with all-in-one plasmids expressing H/F-$mBAZ2A_{WT}$ and H/F-$mBAZ2A_{\Delta TAM}$. BAZ2A signal was detected with anti-HA antibodies. Nucleolin served as a loading control.

c. FACS-sorted, GFP-(+) PC3 cells transfected with all-in-one constructs expressing H/F-mBAZ2A$_{WT}$ and H/F-mBAZ2A$_{\Delta TAM}$ with simultaneous downregulation of endogenous human BAZ2A. qRT-PCR showing mRNA levels of human BAZ2A (left) and total (human and mouse) BAZ2A (right). Control cells were transfected with plasmid for GFP-only expression. mRNA levels were normalized to GAPDH. Error bars represent three independent samples.

d. Sample distances dendrogram of three BAZ2A$_{WT}$ samples (WT1, WT2 and WT3) and three BAZ2A$_{\Delta TAM}$ samples (ΔTAM1, ΔTAM2 and ΔTAM3) using Euclidean distance of the log_2-transformed counts from RNAseq. Dark color indicates higher correlation between the samples.

e. BAZ2A regulates a set of genes in PC3 cells. MA plot of the log_2 fold change of all the genes identified by RNAseq for BAZ2A$_{\Delta TAM}$ in relation to BAZ2A$_{WT}$ in PC3 cells. Blue points depict upregulated (de-repressed) genes with the fold change equal or greater than 1.5 ($log_2FC<0.57$) and red points depict downregulated genes with the fold change equal or less than -1.5 ($log_2FC>0.57$) and *P* value<0.05.

f. BAZ2A regulates the expression of genes frequently repressed in metastatic mPCa through its TAM domain. qRT-PCR showing mRNA levels of the genes frequently repressed in mPCa upon expression of BAZ2A$_{WT}$ and BAZ2A$_{\Delta TAM}$ domain in GFP(+)-FACS-sorted PC3 cells. Control cells were transfected with plasmid for GFP-only expression. mRNA levels were normalized to *GAPDH* and control cells transfected with plasmid expressing GFP. Error bars represent standard deviation of three independent experiments. Statistical significance (*P*-value) was calculated using two-tailed t-test (*<0.05, **<0.01, ***< 0.001, ****<0.0001).

g. Top fifteen biological process gene ontology (GO) terms as determined using DAVID for genes upregulated (de-repressed) and downregulated in PC3 cells expressing BAZ2A$_{\Delta TAM}$ compared to PC3 expressing BAZ2A$_{WT}$.

Figure 3

BAZ2A-TAM domain is required for the repression of a set of genes that have their enhancers bound by BAZ2A

a. Pie charts showing the number of genes in the nearest linear genome proximity to BAZ2A-bound C2 enhancers and their expression changes relative to the expression upon

BAZ2A$_{\Delta TAM}$ compared to PC3 cells expressing BAZ2A$_{WT}$. Genes significantly affected by BAZ2A$_{\Delta TAM}$ expression, log_2 fold change ±0.1, $P < 0.05$.

b. Wiggle tracks showing RNA levels in PC3 cells expressing BAZ2A$_{WT}$ and BAZ2A$_{\Delta TAM}$, occupancy of BAZ2A, C2 enhancer, and its nearest gene *CSF2*.

c. BAZ2A-TAM domain does not affect the association with C2-enhancers. HA-ChIP analysis of PC3 cells transfected with H/F- BAZ2A$_{WT}$ and H/F-BAZ2A$_{\Delta TAM}$ showing the association of BAZ2A with the nearest C2 enhancers (enh.) to genes derepressed by BAZ2A$_{\Delta TAM.}$ The association with the promoter of BAZ2A-regulated gene *AOX1* is also shown. Values were normalized to input and control samples. Values are from two independent experiments. Grey and black dots represent the values obtained from each single experiment.

Figure 4

BAZ2A associates with TOP2A and KDM1A through TAM domain and RNA in PCa cells

a. HA-BAZ2A immunoprecipitation from nuclear extracts of PC3 cells transfected with plasmids expressing H/F-BAZ2A$_{WT}$ and H/F-BAZ2A$_{WY/GA}$. BAZ2A signal was detected with anti-HA antibodies. The interaction with SNF2H was visualized with anti-SNF2H antibodies.

b. Mass spectrometry analysis of H/F-BAZ2A$_{WT}$ and H/F-BAZ2A$_{WY/GA}$ immuno-precipitates from PC3 cells. Values represent average of peptide numbers from three independent experiments. Values in orange represent proteins with decreased association with BAZ2A$_{WY/GA}$ compared to BAZ2A$_{WT}$.

c. STRING analysis depicting functional protein association networks of BAZ2A-interacting proteins that depend on a functional TAM domain.

d. HA-BAZ2A immunoprecipitation of nuclear extracts for PC3 cells transfected with plasmids expressing H/F-BAZ2A$_{WT}$, H/F-BAZ2A$_{WY/GA}$, and H/F-BAZ2A$_{\Delta TAM}$. BAZ2A-intercating proteins are visualized in immunoblots with the corresponding antibodies.

e. TOP2A and KDM1A interactions with BAZ2A depend on RNA. HA-immunoprecipitation from nuclear extract of PC3 cells and the PC3 cell line expressing endogenous BAZ2A with H/F tag that were treated with or without RNase A (0.1μg/μl). BAZ2A-intercating proteins are visualized in immunoblots with the corresponding antibodies.

f. Schema representing the role of BAZ2A-TAM domain and RNA in mediating BAZ2A association with TOP2A, KDM1A, SMC1A, RAD21, and NUP107.

Figure 5

TOP2A and KDM1A activities regulate the expression of BAZ2A-repressed genes in PC3 cells

a,b. Boxplots showing expression profiles of *TOP2A* and *KDM1A* from gene expression microarray GEO data sets GDS2545 and GDS1439 (Chandran et al., 2007; Yu et al., 2004). Statistical significance (*P*-value) was calculated using two-tailed t-test (* <0.05, **<0.01, ****<0.0001); ns, not significant.

c,d. *TOP2A* and *KDM1A* expression levels from metastatic (**c**) and primary (**d**) prostate tumors expressing high low BAZ2A levels. Quartile 1: the top 25% of PCas with the highest BAZ2A expression; quartile 4: the top 25% of PCas with the lowest BAZ2A levels.

e. PCa subtypes and *PTEN* copy number alterations (CNA) in primary PCa groups defined by BAZ2A, TOP2A, and KDM1A expression levels (e.g., quartile Q1: the top 25% of PCas with the highest expression; Q4: the top 25% of PCas with the lowest levels). The molecular subtypes of primary PCa (ERG fusions, ETV1/ETV4/FLI1 fusions, or overexpression, and SPOP/FOXA1/IDH1 mutations) defined in (Cancer Genome Atlas Research, 2015) are shown.

f,g. qRT-PCR showing the mRNA levels of BAZ2A-TAM regulated genes upon inhibition of TOP2A with 10μM ICRF-193 (**e**) and upon inhibition of KDM1A with 10μM OG-L002 (**f**). mRNA levels normalized to *GAPDH* and control cells treated with DMSO. Error bars represent standard deviation of three independent samples. Statistical significance (*P*-value) was calculated using two-tailed t-test (*<0.05, **<0.01, ***< 0.001, ****<0.0001); ns, not significant.

h. Schema representing the role of BAZ2A-TAM and bromodomain (BRD) and RNA in mediating targeting to C2-enhancers containing H3K14ac and the association with TOP2A and KDM1A for the repression of gene expression in PCa cells.

Supplementary Figure

Supplementary Figure S1

Boxplots showing expression profiles of genes were linked to signal transduction, response to wounding and cell migration and motility that are repressed through BAZ2A-TAM domain from the gene expression microarray GEO data set GDS2545 (Chandran et al., 2007; Yu et al., 2004). Statistical significance (*P*-value) was calculated using two-tailed t-test (*<0.05, **<0.01, ***< 0.001, ****<0.0001); ns, not significant.

References

Anosova, I., Melnik, S., Tripsianes, K., Kateb, F., Grummt, I., and Sattler, M. (2015). A novel RNA binding surface of the TAM domain of TIP5/BAZ2A mediates epigenetic regulation of rRNA genes. Nucleic Acids Res *43*, 5208-5220.

Cancer Genome Atlas Research, N. (2015). The Molecular Taxonomy of Primary Prostate Cancer. Cell *163*, 1011-1025.

Chandran, U.R., Ma, C., Dhir, R., Bisceglia, M., Lyons-Weiler, M., Liang, W., Michalopoulos, G., Becich, M., and Monzon, F.A. (2007). Gene expression profiles of prostate cancer reveal involvement of multiple molecular pathways in the metastatic process. BMC Cancer *7*, 64.

Cheville, J.C., Karnes, R.J., Therneau, T.M., Kosari, F., Munz, J.M., Tillmans, L., Basal, E., Rangel, L.J., Bergstralh, E., Kovtun, I.V.*, et al.* (2008). Gene panel model predictive of outcome in men at high-risk of systemic progression and death from prostate cancer after radical retropubic prostatectomy. J Clin Oncol *26*, 3930-3936.

Dalcher, D., Tan, J.Y., Bersaglieri, C., Pena-Hernandez, R., Vollenweider, E., Zeyen, S., Schmid, M.W., Bianchi, V., Butz, S., Roganowicz, M.*, et al.* (2020). BAZ2A safeguards genome architecture of ground-state pluripotent stem cells. EMBO J *39*, e105606.

de Dieuleveult, M., Yen, K., Hmitou, I., Depaux, A., Boussouar, F., Bou Dargham, D., Jounier, S., Humbertclaude, H., Ribierre, F., Baulard, C.*, et al.* (2016). Genome-wide nucleosome specificity and function of chromatin remodellers in ES cells. Nature *530*, 113-116.

de Resende, M.F., Vieira, S., Chinen, L.T., Chiappelli, F., da Fonseca, F.P., Guimarães, G.C., Soares, F.A., Neves, I., Pagotty, S., Pellionisz, P.A.*, et al.* (2013). Prognostication of prostate cancer based on TOP2A protein and gene assessment: TOP2A in prostate cancer. J Transl Med *11*, 36.

Etani, T., Naiki, T., Naiki-Ito, A., Suzuki, T., Iida, K., Nozaki, S., Kato, H., Nagayasu, Y., Suzuki, S., Kawai, N.*, et al.* (2019). NCL1, A Highly Selective Lysine-Specific Demethylase 1 Inhibitor, Suppresses Castration-Resistant Prostate Cancer Growth via Regulation of Apoptosis and Autophagy. J Clin Med *8*.

Gu, L., Frommel, S.C., Oakes, C.C., Simon, R., Grupp, K., Gerig, C.Y., Bar, D., Robinson, M.D., Baer, C., Weiss, M.*, et al.* (2015). BAZ2A (TIP5) is involved in epigenetic alterations in prostate cancer and its overexpression predicts disease recurrence. Nat Genet *47*, 22-30.

Guetg, C., Scheifele, F., Rosenthal, F., Hottiger, M.O., and Santoro, R. (2012). Inheritance of Silent rDNA Chromatin Is Mediated by PARP1 via Noncoding RNA. Mol Cell *45*, 790-800.

Hanahan, D., and Weinberg, R.A. (2011). Hallmarks of cancer: the next generation. Cell *144*, 646-674.

He, C., Sidoli, S., Warneford-Thomson, R., Tatomer, D.C., Wilusz, J.E., Garcia, B.A., and Bonasio, R. (2016). High-Resolution Mapping of RNA-Binding Regions in the Nuclear Proteome of Embryonic Stem Cells. Mol Cell *64*, 416-430.

Huang da, W., Sherman, B.T., and Lempicki, R.A. (2009). Systematic and integrative analysis of large gene lists using DAVID bioinformatics resources. Nature protocols *4*, 44-57.

Hughes, C., Murphy, A., Martin, C., Fox, E., Ring, M., Sheils, O., Loftus, B., and O'Leary, J. (2006). Topoisomerase II-alpha expression increases with increasing Gleason score and with hormone insensitivity in prostate carcinoma. Journal of clinical pathology *59*, 721-724.

Kahl, P., Gullotti, L., Heukamp, L.C., Wolf, S., Friedrichs, N., Vorreuther, R., Solleder, G., Bastian, P.J., Ellinger, J., Metzger, E.*, et al.* (2006). Androgen receptor coactivators lysine-specific histone demethylase 1 and four and a half LIM domain protein 2 predict risk of prostate cancer recurrence. Cancer research *66*, 11341-11347.

Kashyap, V., Ahmad, S., Nilsson, E.M., Helczynski, L., Kenna, S., Persson, J.L., Gudas, L.J., and Mongan, N.P. (2013). The lysine specific demethylase-1 (LSD1/KDM1A) regulates VEGF-A expression in prostate cancer. Mol Oncol *7*, 555-566.

Labbé, D.P., Sweeney, C.J., Brown, M., Galbo, P., Rosario, S., Wadosky, K.M., Ku, S.-Y., Sjöström, M., Alshalalfa, M., Erho, N., *et al.* (2017a). TOP2A and EZH2 Provide Early Detection of an Aggressive Prostate Cancer Subgroup. Clinical Cancer Research *23*, 7072-7083.

Labbé, D.P., Sweeney, C.J., Brown, M., Galbo, P., Rosario, S., Wadosky, K.M., Ku, S.Y., Sjöström, M., Alshalalfa, M., Erho, N., *et al.* (2017b). TOP2A and EZH2 Provide Early Detection of an Aggressive Prostate Cancer Subgroup. Clinical cancer research : an official journal of the American Association for Cancer Research *23*, 7072-7083.

Lee, F.C.Y., and Ule, J. (2018). Advances in CLIP Technologies for Studies of Protein-RNA Interactions. Mol Cell *69*, 354-369.

Leone, S., Bar, D., Slabber, C.F., Dalcher, D., and Santoro, R. (2017). The RNA helicase DHX9 establishes nucleolar heterochromatin, and this activity is required for embryonic stem cell differentiation. EMBO Rep *18*, 1248-1262.

Li, J.J., and Shen, M.M. (2018). Prostate Stem Cells and Cancer Stem Cells. Cold Spring Harbor Perspectives in Medicine.

Li, X., Liu, Y., Chen, W., Fang, Y., Xu, H., Zhu, H.H., Chu, M., Li, W., Zhuang, G., and Gao, W.Q. (2014). TOP2Ahigh is the phenotype of recurrence and metastasis whereas TOP2Aneg cells represent cancer stem cells in prostate cancer. Oncotarget *5*, 9498-9513.

Liang, Y., Ahmed, M., Guo, H., Soares, F., Hua, J.T., Gao, S., Lu, C., Poon, C., Han, W., Langstein, J., *et al.* (2017). LSD1-Mediated Epigenetic Reprogramming Drives CENPE Expression and Prostate Cancer Progression. Cancer research *77*, 5479-5490.

Liao, Y., Smyth, G.K., and Shi, W. (2013). The Subread aligner: fast, accurate and scalable read mapping by seed-and-vote. Nucleic Acids Res *41*, e108.

Maiques-Diaz, A., and Somervaille, T.C. (2016). LSD1: biologic roles and therapeutic targeting. Epigenomics *8*, 1103-1116.

Mayer, C., Schmitz, K.M., Li, J., Grummt, I., and Santoro, R. (2006). Intergenic transcripts regulate the epigenetic state of rRNA genes. Molecular cell *22*, 351-361.

Mullari, M., Lyon, D., Jensen, L.J., and Nielsen, M.L. (2017). Specifying RNA-Binding Regions in Proteins by Peptide Cross-Linking and Affinity Purification. J Proteome Res *16*, 2762-2772.

Peña-Hernández, R., Aprigliano, R., Frommel, S., Pietrzak, K., Steiger, S., Roganowicz, M., Bizzarro, J., and Santoro, R. (2021). BAZ2A association with H3K14ac is required for the transition of prostate cancer cells into a cancer stem-like state. bioRxiv, 2020.2007.2003.185843.

Perez-Perri, J.I., Rogell, B., Schwarzl, T., Stein, F., Zhou, Y., Rettel, M., Brosig, A., and Hentze, M.W. (2018). Discovery of RNA-binding proteins and characterization of their dynamic responses by enhanced RNA interactome capture. Nat Commun *9*, 4408.

Pietrzak, K., Kuzyakiv, R., Simon, R., Bolis, M., Bar, D., Aprigliano, R., Theurillat, J.P., Sauter, G., and Santoro, R. (2020). TIP5 primes prostate luminal cells for the oncogenic transformation mediated by PTEN-loss. Proc Natl Acad Sci U S A *117*, 3637-3647.

Robinson, D., Van Allen, E.M., Wu, Y.M., Schultz, N., Lonigro, R.J., Mosquera, J.M., Montgomery, B., Taplin, M.E., Pritchard, C.C., Attard, G., *et al.* (2015). Integrative clinical genomics of advanced prostate cancer. Cell *161*, 1215-1228.

Robinson, M.D., and Oshlack, A. (2010). A scaling normalization method for differential expression analysis of RNA-seq data. Genome Biol *11*, R25.

Rudolph, T., Beuch, S., and Reuter, G. (2013). Lysine-specific histone demethylase LSD1 and the dynamic control of chromatin. Biological chemistry *394*, 1019-1028.

Santoro, R., Li, J., and Grummt, I. (2002). The nucleolar remodeling complex NoRC mediates heterochromatin formation and silencing of ribosomal gene transcription. Nat Genet *32*, 393-396.

Savic, N., Bar, D., Leone, S., Frommel, S.C., Weber, F.A., Vollenweider, E., Ferrari, E., Ziegler, U., Kaech, A., Shakhova, O.*, et al.* (2014). lncRNA Maturation to Initiate Heterochromatin Formation in the Nucleolus Is Required for Exit from Pluripotency in ESCs. Cell Stem Cell *15*, 720-734.

Schaefer-Klein, J.L., Murphy, S.J., Johnson, S.H., Vasmatzis, G., and Kovtun, I.V. (2015). Topoisomerase 2 Alpha Cooperates with Androgen Receptor to Contribute to Prostate Cancer Progression. PLoS One *10*, e0142327.

Schmid, M.W., and Grossniklaus, U. (2015). Rcount: simple and flexible RNA-Seq read counting. Bioinformatics *31*, 436-437.

Sehrawat, A., Gao, L., Wang, Y., Bankhead, A., 3rd, McWeeney, S.K., King, C.J., Schwartzman, J., Urrutia, J., Bisson, W.H., Coleman, D.J.*, et al.* (2018). LSD1 activates a lethal prostate cancer gene network independently of its demethylase function. Proceedings of the National Academy of Sciences of the United States of America *115*, E4179-e4188.

Siegel, R.L., Miller, K.D., and Jemal, A. (2015). Cancer statistics, 2015. CA: a cancer journal for clinicians *65*, 5-29.

Strohner, R., Nemeth, A., Jansa, P., Hofmann-Rohrer, U., Santoro, R., Langst, G., and Grummt, I. (2001). NoRC--a novel member of mammalian ISWI-containing chromatin remodeling machines. EMBO J *20*, 4892-4900.

Sung, H., Ferlay, J., Siegel, R.L., Laversanne, M., Soerjomataram, I., Jemal, A., and Bray, F. (2021). Global cancer statistics 2020: GLOBOCAN estimates of incidence and mortality worldwide for 36 cancers in 185 countries. CA Cancer J Clin.

Szklarczyk, D., Franceschini, A., Wyder, S., Forslund, K., Heller, D., Huerta-Cepas, J., Simonovic, M., Roth, A., Santos, A., Tsafou, K.P.*, et al.* (2015). STRING v10: protein-protein interaction networks, integrated over the tree of life. Nucleic Acids Res *43*, D447-452.

Tsai, M.C., Manor, O., Wan, Y., Mosammaparast, N., Wang, J.K., Lan, F., Shi, Y., Segal, E., and Chang, H.Y. (2010). Long noncoding RNA as modular scaffold of histone modification complexes. Science *329*, 689-693.

Yadav, S.S., Stockert, J.A., Hackert, V., Yadav, K.K., and Tewari, A.K. (2018). Intratumor heterogeneity in prostate cancer. Urologic Oncology: Seminars and Original Investigations *36*, 349-360.

Yang, C., Wang, W., Liang, J.-X., Li, G., Vellaisamy, K., Wong, C.-Y., Ma, D.-L., and Leung, C.-H. (2017). A Rhodium(III)-Based Inhibitor of Lysine-Specific Histone Demethylase 1 as an Epigenetic Modulator in Prostate Cancer Cells. Journal of Medicinal Chemistry *60*, 2597-2603.

Yu, Y.P., Landsittel, D., Jing, L., Nelson, J., Ren, B., Liu, L., McDonald, C., Thomas, R., Dhir, R., Finkelstein, S.*, et al.* (2004). Gene expression alterations in prostate cancer predicting tumor aggression and preceding development of malignancy. Journal of clinical oncology : official journal of the American Society of Clinical Oncology *22*, 2790-2799.

Zhong, Z., Yu, J., Virshup, D.M., and Madan, B. (2020). Wnts and the hallmarks of cancer. Cancer metastasis reviews *39*, 625-645.

Figure 1

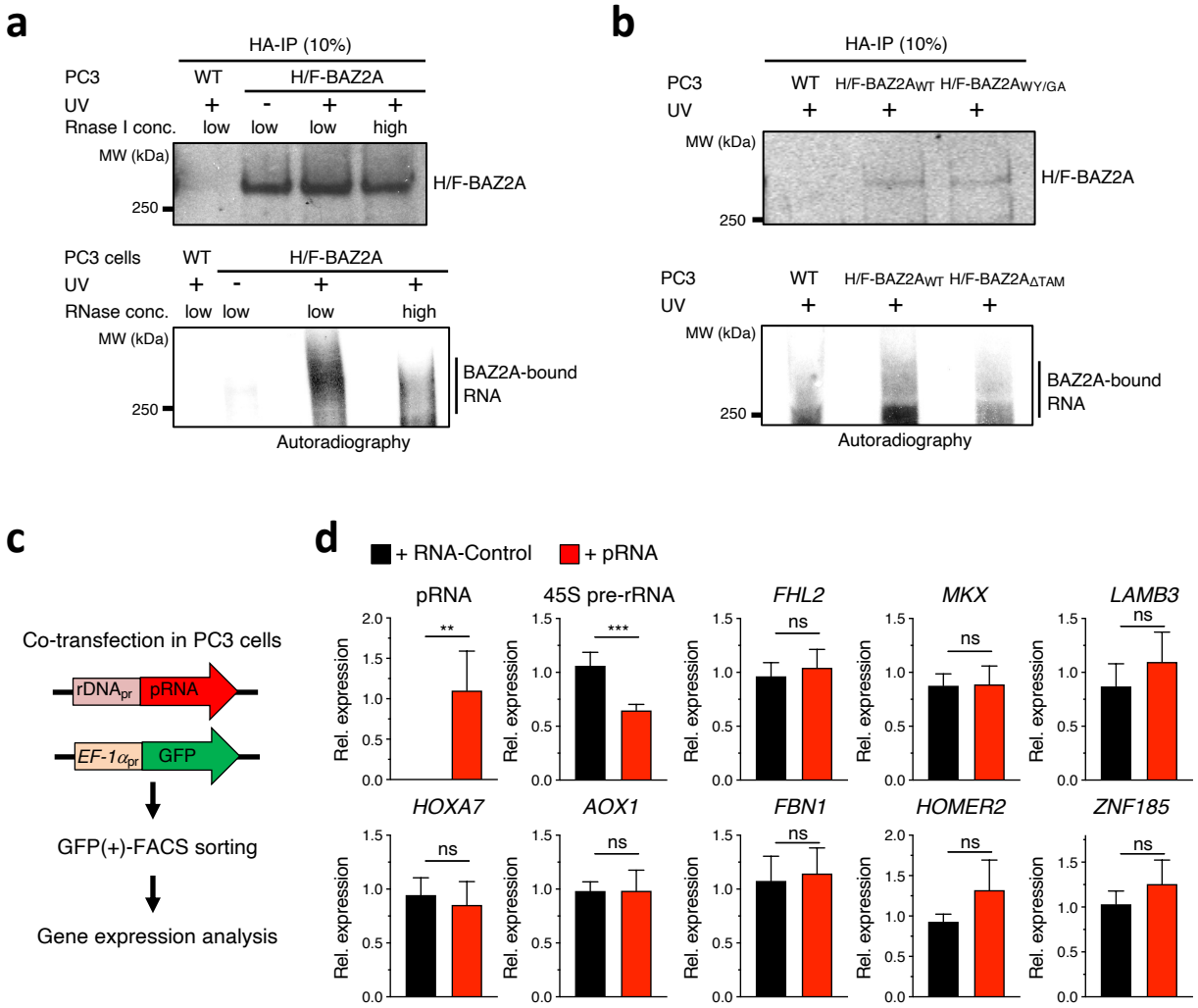
a
HA-IP (10%)
PC3
WT
H/F-BAZ2A
UV
+
-
+
+
Rnase I conc.
low
low
low
high
MW (kDa)
250
H/F-BAZ2A
PC3 cells
WT
H/F-BAZ2A
UV
+
-
+
+
RNase conc.
low
low
low
high
MW (kDa)
250
BAZ2A-bound RNA
Autoradiography
b
HA-IP (10%)
PC3
WT
H/F-BAZ2AWT
H/F-BAZ2AWY/GA
UV
+
+
+
MW (kDa)
250
H/F-BAZ2A
PC3
WT
H/F-BAZ2AWT
H/F-BAZ2AΔTAM
UV
+
+
+
MW (kDa)
250
BAZ2A-bound RNA
Autoradiography
c
Co-transfection in PC3 cells
rDNApr
pRNA
EF-1αpr
GFP
GFP(+)-FACS sorting
Gene expression analysis
d
+ RNA-Control
+ pRNA
pRNA
45S pre-rRNA
FHL2
MKX
LAMB3
HOXA7
AOX1
FBN1
HOMER2
ZNF185
Rel. expression
**
***
ns

Figure 2

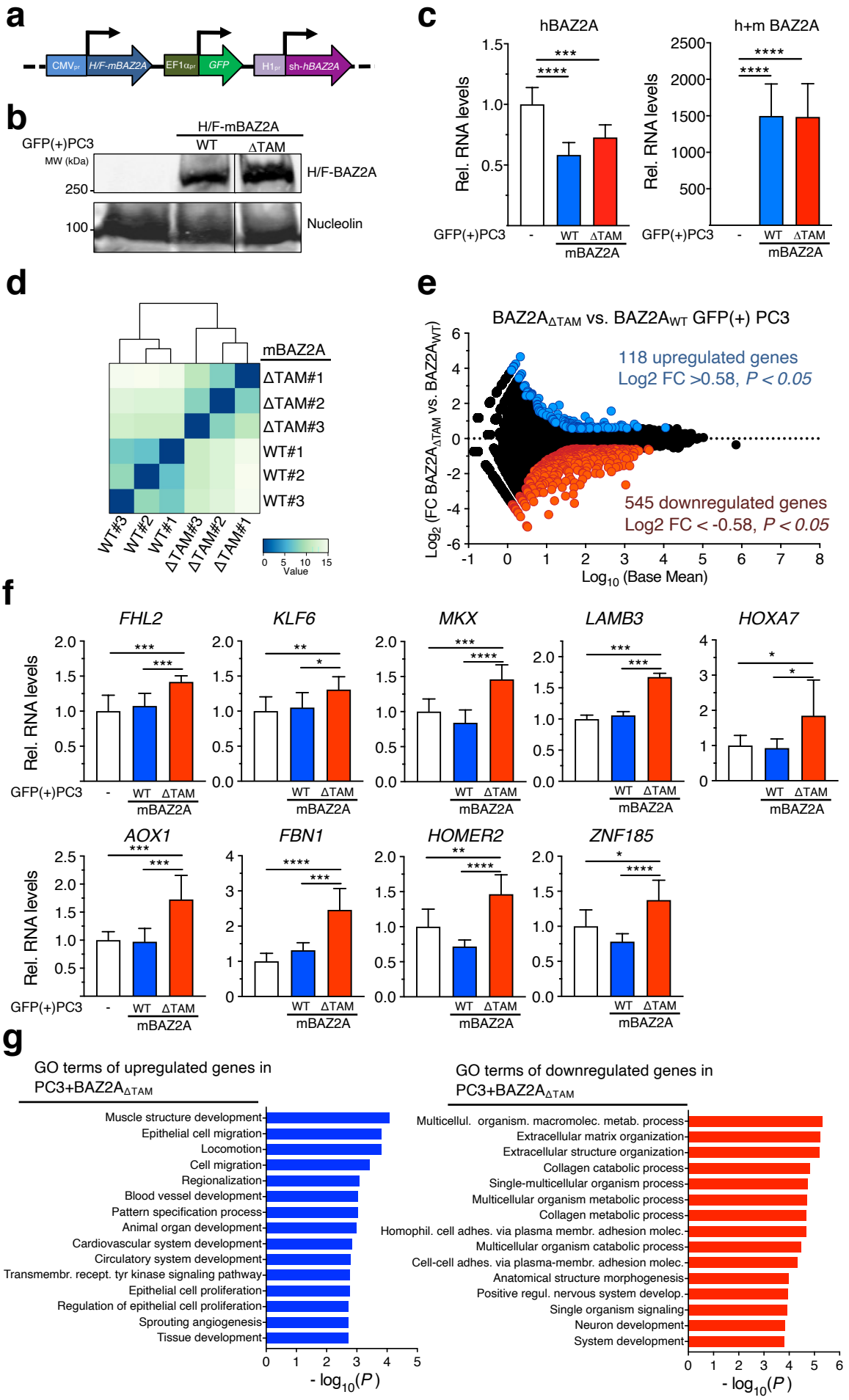
a
CMVpr
H/F-mBAZ2A
EF1αpr
GFP
H1pr
sh-hBAZ2A
b
GFP(+)PC3
H/F-mBAZ2A
WT
ΔTAM
MW (kDa)
250
100
H/F-BAZ2A
Nucleolin
c
hBAZ2A
h+m BAZ2A
Rel. RNA levels
GFP(+)PC3
-
WT
ΔTAM
mBAZ2A
d
mBAZ2A
ΔTAM#1
ΔTAM#2
ΔTAM#3
WT#1
WT#2
WT#3
Value
e
BAZ2AΔTAM vs. BAZ2AWT GFP(+) PC3
118 upregulated genes
Log2 FC >0.58, P < 0.05
545 downregulated genes
Log2 FC < -0.58, P < 0.05
Log2 (FC BAZ2AΔTAM vs. BAZ2AWT)
Log10 (Base Mean)
f
FHL2
KLF6
MKX
LAMB3
HOXA7
AOX1
FBN1
HOMER2
ZNF185
g
GO terms of upregulated genes in PC3+BAZ2AΔTAM
Muscle structure development
Epithelial cell migration
Locomotion
Cell migration
Regionalization
Blood vessel development
Pattern specification process
Animal organ development
Cardiovascular system development
Circulatory system development
Transmembr. recept. tyr kinase signaling pathway
Epithelial cell proliferation
Regulation of epithelial cell proliferation
Sprouting angiogenesis
Tissue development
- log10(P)
GO terms of downregulated genes in PC3+BAZ2AΔTAM
Multicellul. organism. macromolec. metab. process
Extracellular matrix organization
Extracellular structure organization
Collagen catabolic process
Single-multicellular organism process
Multicellular organism metabolic process
Collagen metabolic process
Homophil. cell adhes. via plasma membr. adhesion molec.
Multicellular organism catabolic process
Cell-cell adhes. via plasma-membr. adhesion molec.
Anatomical structure morphogenesis
Positive regul. nervous system develop.
Single organism signaling
Neuron development
System development
- log10(P)

Figure 3

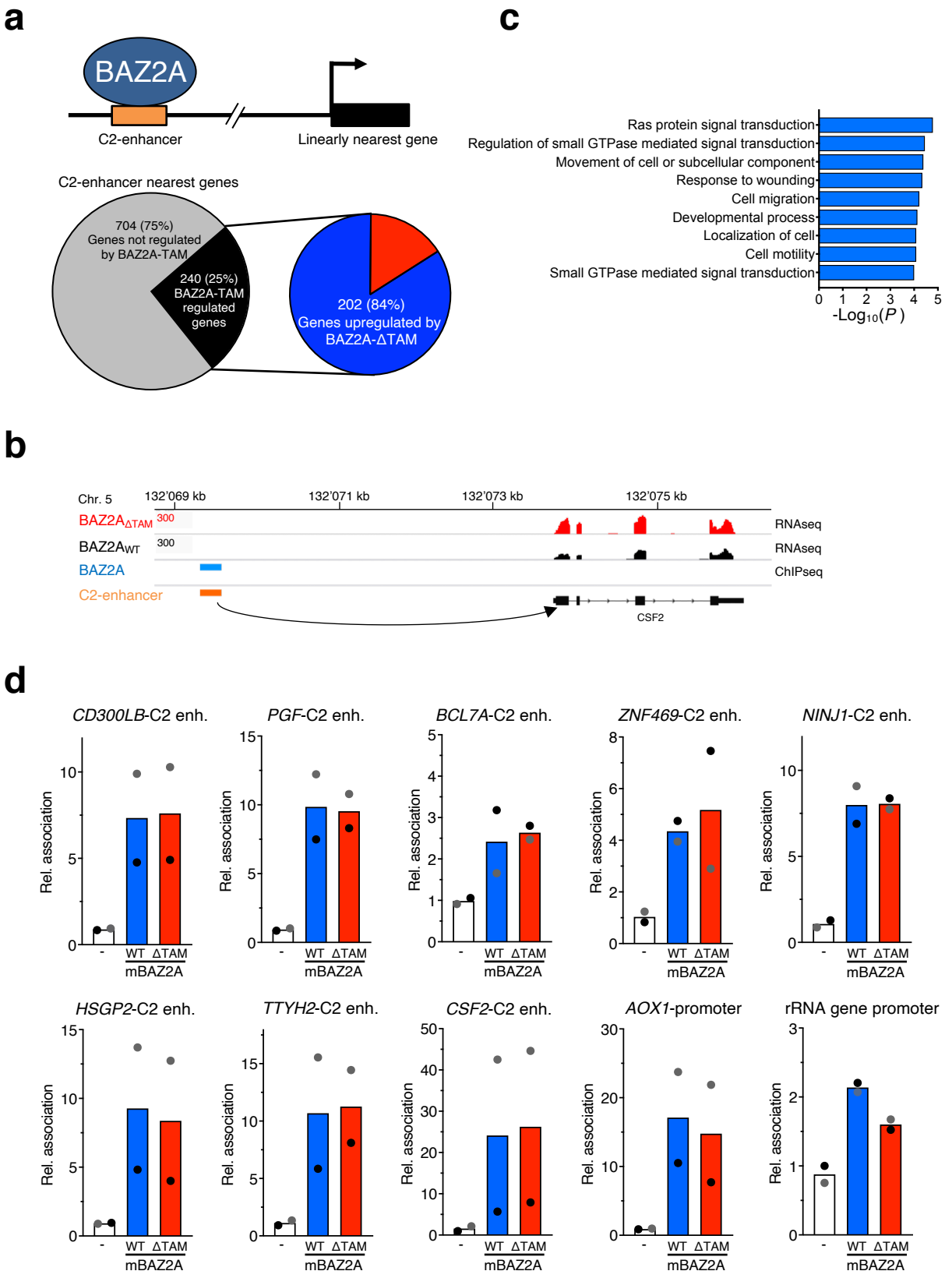
a
BAZ2A
C2-enhancer
Linearly nearest gene
C2-enhancer nearest genes
704 (75%)
Genes not regulated
by BAZ2A-TAM
240 (25%)
BAZ2A-TAM
regulated
genes
202 (84%)
Genes upregulated by
BAZ2A-ΔTAM
c
Ras protein signal transduction
Regulation of small GTPase mediated signal transduction
Movement of cell or subcellular component
Response to wounding
Cell migration
Developmental process
Localization of cell
Cell motility
Small GTPase mediated signal transduction
0 1 2 3 4 5
-Log10(P)
b
Chr. 5
132'069 kb
132'071 kb
132'073 kb
132'075 kb
BAZ2AΔTAM
BAZ2AWT
BAZ2A
C2-enhancer
300
300
RNAseq
RNAseq
ChIPseq
CSF2
d
CD300LB-C2 enh.
PGF-C2 enh.
BCL7A-C2 enh.
ZNF469-C2 enh.
NINJ1-C2 enh.
HSGP2-C2 enh.
TTYH2-C2 enh.
CSF2-C2 enh.
AOX1-promoter
rRNA gene promoter
Rel. association
- WT ΔTAM
mBAZ2A

Figure 4

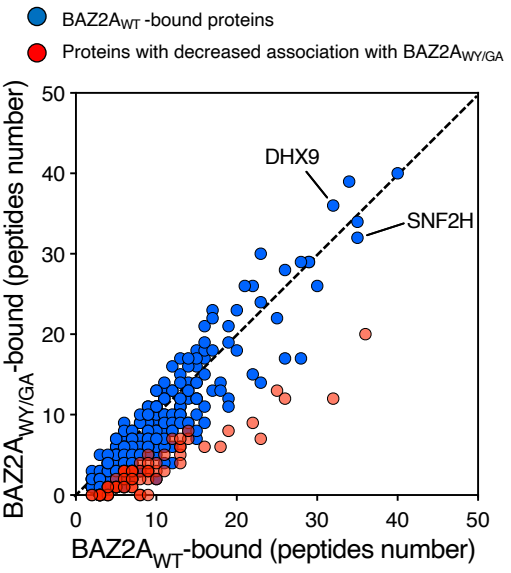

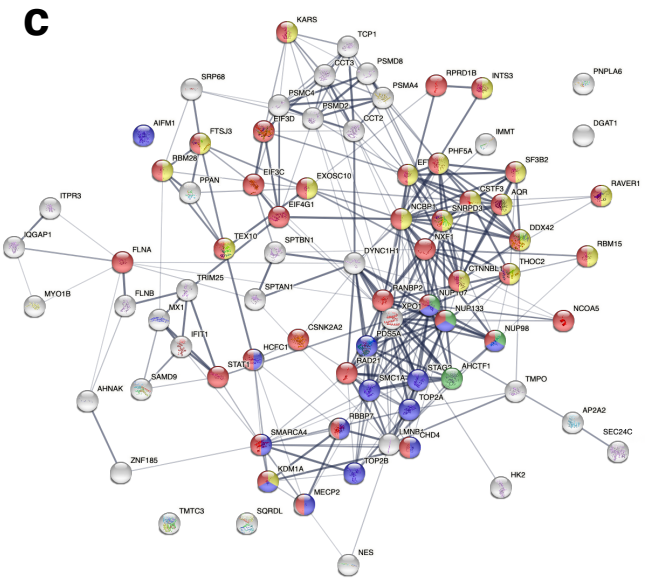

Biological processes	FDR
Gene expression	9.4×10^{-7}
Chromosome organization	3.6×10^{-4}
Nuclear pore organization	5.3×10^{-5}
RNA processing	2.4×10^{-7}

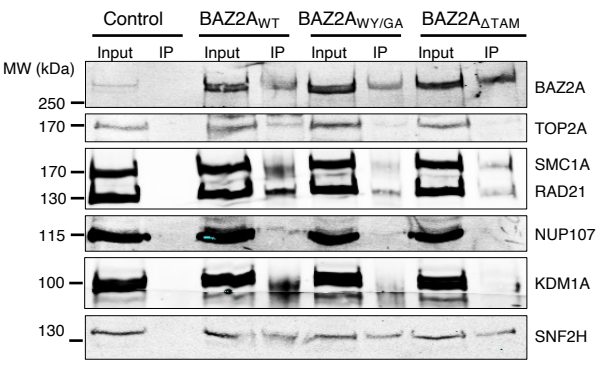

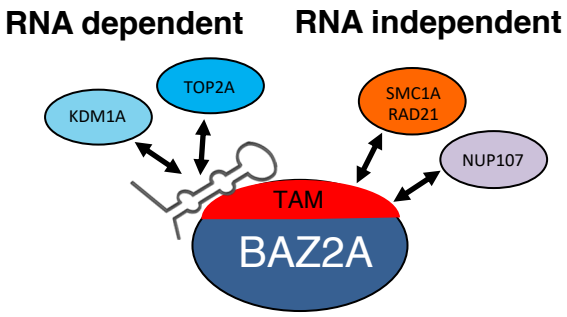

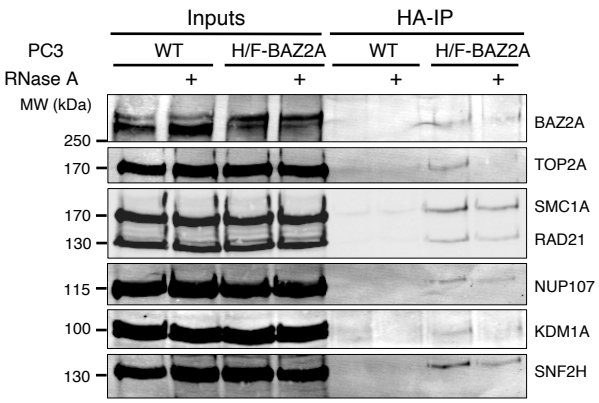

Figure 5

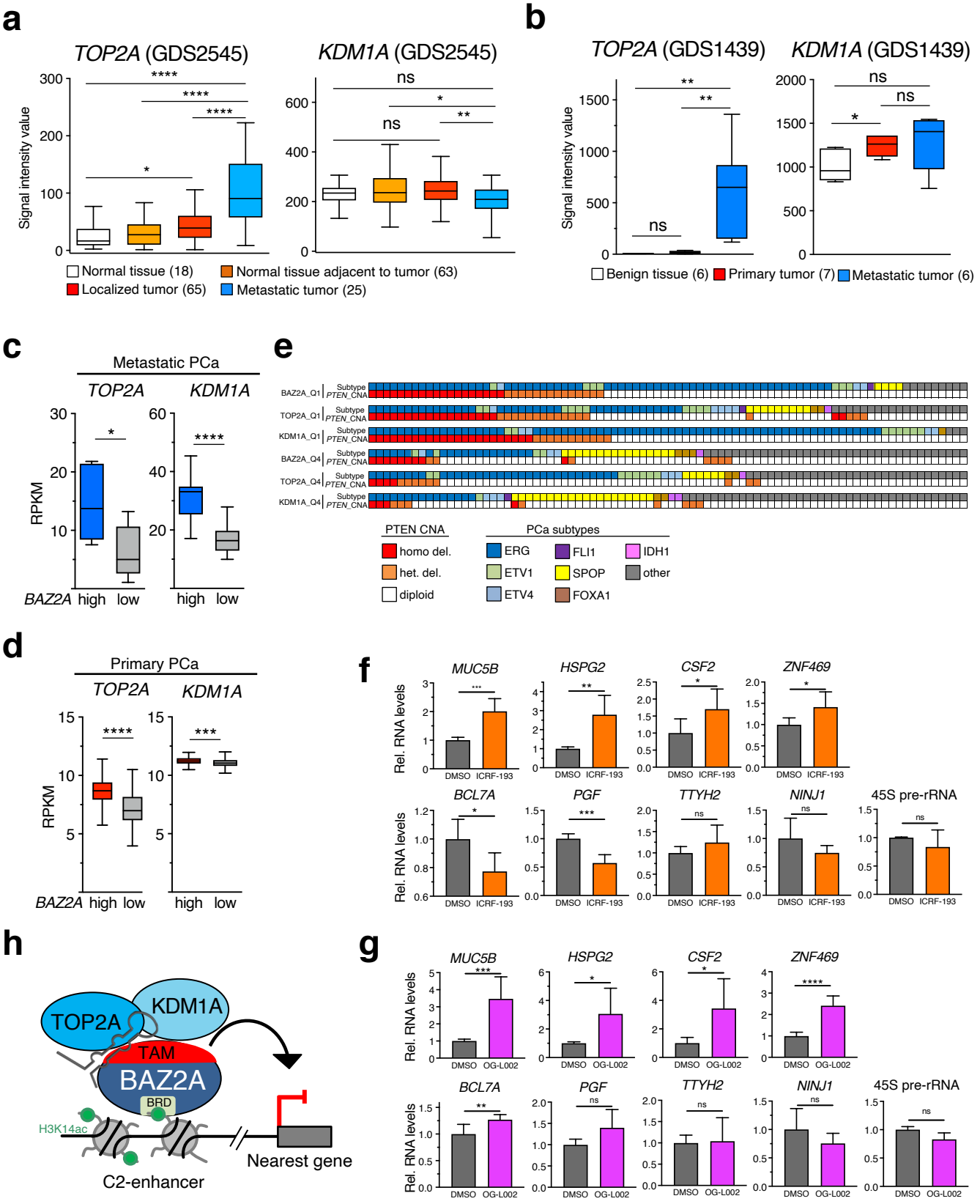
a
TOP2A (GDS2545)
KDM1A (GDS2545)
Signal intensity value
Normal tissue (18)
Normal tissue adjacent to tumor (63)
Localized tumor (65)
Metastatic tumor (25)
b
TOP2A (GDS1439)
KDM1A (GDS1439)
Benign tissue (6)
Primary tumor (7)
Metastatic tumor (6)
c
Metastatic PCa
TOP2A
KDM1A
RPKM
BAZ2A high low
e
PTEN CNA
homo del.
het. del.
diploid
PCa subtypes
ERG
ETV1
ETV4
FLI1
SPOP
FOXA1
IDH1
other
d
Primary PCa
f
MUC5B
HSPG2
CSF2
ZNF469
BCL7A
PGF
TTYH2
NINJ1
45S pre-rRNA
Rel. RNA levels
DMSO
ICRF-193
h
TOP2A
KDM1A
TAM
BAZ2A
BRD
H3K14ac
C2-enhancer
Nearest gene
g
OG-L002